The College of Engineering
University of Wisconsin-Madison

Wisconsin Electric Machines and Power Electronics Consortium

RESEARCH REPORT
92-37

A Novel Permanent Magnet Motor with Doubly Salient Structure

Yuefeng Liao, Feng Liang and Thomas A. Lipo
Dept. of Electrical and Computer Engineering
University of Wisconsin-Madison
1415 Johnson Drive
Madison, WI 53706

WEMPEC

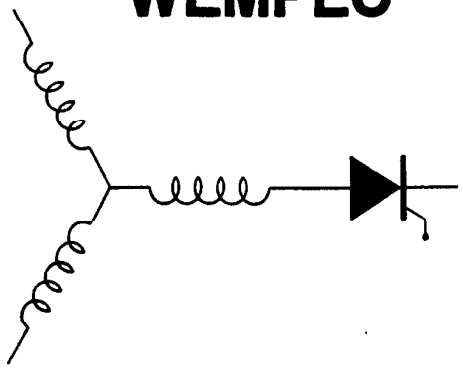

Department of Electrical and Computer Engineering
1415 Johnson Drive
Madison, Wisconsin 53706

A Novel Permanent Magnet Motor with Doubly Salient Structure

Yuefeng Liao, Feng Liang and Thomas A. Lipo
Department of Electrical and Computer Engineering
University of Wisconsin-Madison
1415 Johnson Drive
Madison, WI 53706-1691

Abstract - **A new type of doubly salient machine is presented in which the field excitation is provided by non-rotating Permanent Magnet. This doubly salient permanent magnet (DSPM) motor is shown to be kindred to square waveform permanent magnet brushless DC (PM-BLDC) motors. Linear and nonlinear analysis has been made to investigate the characteristics of this new type of PM motor. A prototype DSPM motor is designed and comparison made between this new type of motor and the induction motor. It is shown that by fully exploiting modern high energy PM material and the doubly salient structure, the DSPM motor can offer superior performance over existing motors in terms of efficiency, torque density, torque-to-current ratio, torque-to-inertia ratio etc. while retaining a simple structure amenable to automatic manufacture.**

I. INTRODUCTION

The Variable Reluctance Motor (VRM) employing a doubly salient structure has been the focus of intensive research efforts during the past decade and its torque production, design features and control characteristics have been well explored [1-4]. In particular, the inherent fault-tolerant feature of this machine, among other merits claimed by its proponents, has been well demonstrated, and the variable reluctance motor is becoming a prime candidate for reliability-premium applications [5].

The VRM is, fundamentally, one of a class of singly-excited electro-mechanical energy conversion devices. Unlike doubly-excited electrical machines, the lack of a separate field winding in the VRM contributes to the structural simplicity and the inherent high reliability of the VRM drive. However, this feature also gives rise to a number of problems as viewed from the point of view of energy conversion. Firstly, the variable reluctance action necessitates the use of only one of two possible torque producing zones. That is, motoring torque can be produced only when a rotor pole is entering the region occupied by a given phase, i.e. when the inductance is increasing. Only braking torque can be produced if the phase is energized while the pole is leaving the aligned, maximum inductance position. Utilization of the active copper and iron materials within the machine is thus relatively poor in the VRM. Secondly, the VRM essentially operates in a mode in which the field energy is first supplied to and then withdrawn from the machine one phase at a time. No sooner is the field energy supplied to the machine, than it must be rapidly withdrawn from each phase just as the phase inductance is reaching its maximum, in order to prevent drawing energy from the mechanical system (i.e. producing negative torque). The problem with this limitation lies in the large turn-off inductance, which prevents the current from dropping quickly. This problem of current commutation associated with a large turn-off inductance greatly decreases the torque production capability of the VRM fed by a non-ideal power converter with finite KVA. This feature can be viewed as an additional penalty to the "excitation penalty" normally imposed on all electrically excited machines, particularly for small machines. The excitation penalty relates to the fact that the phases of electrically excited machines must not only carry the torque producing component of current but must also support the excitation component which serves to magnetize the machine. As a result, both the machine windings and the power converter are usually highly stressed from the point of view of voltage and current, resulting in the need for an increased VA rating for the drive. Also, the airgap of the VRM must be substantially reduced compared to other competing machines to help push the machine into the highly saturated region. This requirement adversely offsets the potential low cost advantage of the VRM in addition to causing acoustic noise and torque pulsation. Despite extensive efforts directed at dealing with these practicalities [6], the VRM has thus far fallen short of its theoretical potential in terms of torque density, efficiency and converter VA rating. As a result, many researchers view present VRM technology with some skepticism.

Recently, Philips proposed the use of an additional full-pitched winding in the VRM to act as a field winding in an attempt to improve its torque production, based on the concept of pre-magnetization [7-8]. The machine of Philips is, in reality, a single stack homopolar inductor machine fed from an unipolar converter, with the field excitation provided by the full-pitched winding. This machine configuration has also been explored by the authors from a different perspective [9]. Similar work can be found in an earlier implementation of the concept of pre-magnetization by Torok in a family of multiphase reluctance machines he invented [10]. All these machines can be viewed as field-assisted variable reluctance machines, with energy converted primarily through reluctance torque. However, both Philips and Torok failed to recognize the uniqueness brought about by the possible use of PM excitation.

This paper presents a new type of doubly salient motor in which the field excitation is supplied by Permanent Magnet installed in the either the stator or rotor of the motor. This new type of PM motor has evolved from the

0-7803-0634-1/92S03.00 ©IEEE

doubly salient homopolar inductor machine [11] and is therefore termed the doubly salient permanent magnet (DSPM) motor. It will be shown that by introducing modern high performance permanent magnet to advantage in such machines, the above mentioned deficiencies of the VRM are virtually eliminated. The torque production of this motor can then be greatly enhanced. The penalty paid, though, is the need for expensive PM material and the loss of the fault-tolerance feature. This newly conceived DSPM motor can take on homopolar, rotary magnet and stationary magnet structures [12-13]. This paper will focus on the DSPM motor with stationary PM, while the rotary magnet version of the DSPM motor has been described in a previous paper [14]. A discussion of the homopolar version is forthcoming.

II. BASIC PRINCIPLES OF OPERATION AND CONTROL

2.1 Configuration of the DSPM Machine

Figure 1 shows the cross-section of a 3-phase, 6/4-pole DSPM motor with stationary magnets. This 3-phase, 6/4-pole configuration is the most simple pattern for motoring operation requiring satisfactory starting performance. However, two phase or even single phase schemes can be conceived for use as a generator. For low speed and high torque applications, the machine can be constructed in repetitive fashion, for example a 12/8 pole configuration.

It can be noted that the rotor of the DSPM machine is identical to that of the three phase variable reluctance machine. The stator structure is also similar to that of the VRM except that two pieces of PM are buried in the core and therefore introduced into the main flux path of the stator windings. In order to achieve a high flux concentration in such machines, use is made of the corners of the stator lamination which are normally discarded. This changes the physical appearance of the motor to either a square or "football" shaped cross-section and adds slightly to the weight and space occupied by the machine. High performance PM material with a linear demagnetizing characteristic is used to sustain the magnetization and demagnetization of the armature reaction so as to keep a nearly constant flux level within the air gap. The stator pole arc is set to be $\pi/6$ mechanical radians and the rotor pole arc selected to be slightly greater than the stator pole arc to allow for current reversal. As configured, the airgap reluctance, seen by the PM excitation is invariant of rotor position if fringing is negligible. Therefore, there is essentially no cogging torque produced at no-load. A linear variation of the PM induced flux linkage and thus a trapezoidal back EMF is induced in each of the stator windings at no-load as shown in Fig. 1.

When the machine is loaded, armature reaction flux is produced in the windings in addition to the PM induced flux. It is important to note, however, that the existence of the PM constitutes a very high reluctance path for the armature reaction flux and thus forces the bulk of the armature reaction flux to circulate through another overlapped pole pair. As a result, the active stator phase winding will possess small inductances at both aligned and unaligned positions, and the maximum inductance appears when the poles is, in fact, essentially half overlapped, as illustrated in Fig. 2. In contrast to the VRM this small aligned inductance makes it possible to reverse the current

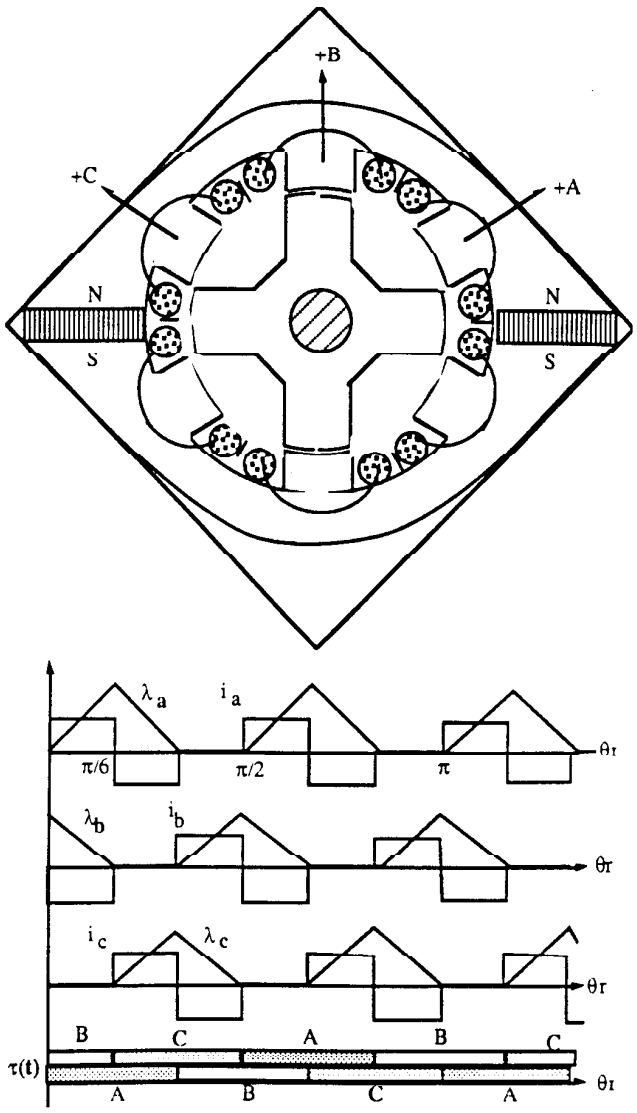

Fig. 1 Illustration of Operating Principles of the DSPM Motor

rapidly at the aligned position. Therefore, torque can be produced both by applying positive current to the winding when its PM-induced flux is increasing and by applying negative current while the flux is decreasing, as shown in Fig. 1.

2.2 Torque Production in the DSPM Machine

The torque expression derived below is based on a simplified linear model for the purpose of illustration. As a first approximation, the variation of the winding inductance and the PM induced flux linkage of an active stator phase winding are assumed to be piece-wise linear and spatially dependent only, as shown in Fig. 2. The terminal voltage equation for an active stator phase winding is then

$$v = Ri + e \approx e = \frac{d\psi}{dt} \qquad (1)$$

The flux linkage ψ is composed of the PM induced flux linkage ψ_m and the armature reaction flux linkage (Li):

$$\psi = Li + \psi_m \qquad (2)$$

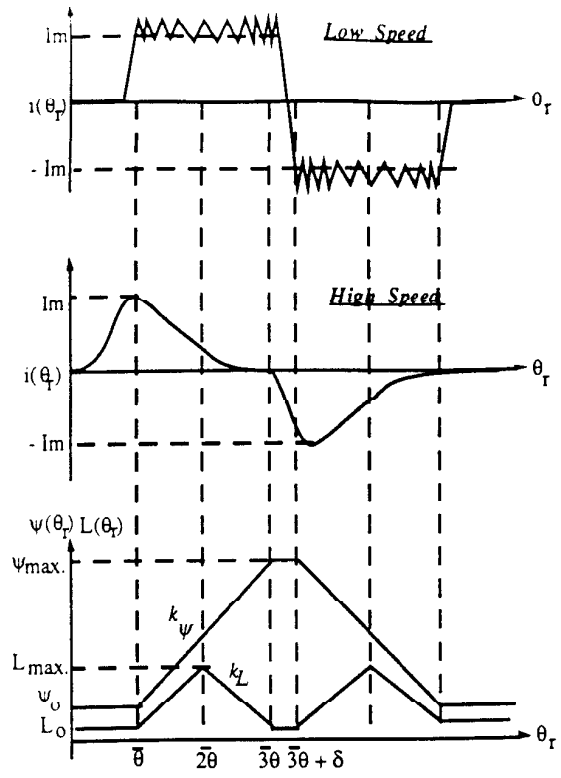

Fig. 2 Current Waveforms of the DSPM Motor

Therefore,

$$e = \frac{d\psi}{dt} = L\frac{di}{dt} + i\frac{dL}{dt} + \frac{d\psi_m}{dt}$$
$$= L\frac{di}{dt} + e_r + e_m \qquad (3)$$

This result suggests the equivalent circuit of Fig. 3.

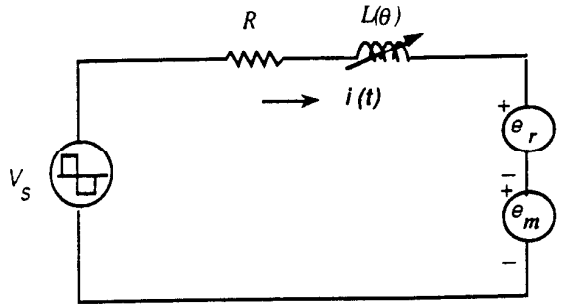

Fig. 3 Equivalent Circuit of the DSPM Motor

The electrical power entering any of the windings is, neglecting ohmic and iron losses,

$$P_e = ei = iL\frac{di}{dt} + i^2\frac{dL}{dt} + i\frac{d\psi_m}{dt}$$

$$= \frac{d}{dt}\left(\frac{1}{2}Li^2\right) + \left(\frac{1}{2}i^2\frac{\partial L}{\partial \theta_r} + i\frac{\partial \psi_m}{\partial \theta_r}\right)\omega_r \qquad (4)$$

Power balance gives

$$P_e = \frac{d}{dt}W_f + T\omega_r \qquad (5)$$

Hence, the torque can be written as the sum of two components

$$T = \frac{1}{2}i^2\frac{\partial L}{\partial \theta_r} + i\frac{\partial \psi_m}{\partial \theta_r}$$
$$= T_r + T_m \qquad (6)$$

while the field energy is

$$W_f = \frac{1}{2}Li^2 \qquad (7)$$

Careful examination of (6) and (7) reveals the following features of the DSPM motor:

(i) The reaction torque T_m, which is the dominant torque component, can be produced by applying either a positive current to a phase winding when its flux linkage is increasing ($e_m > 0$) or a negative current when the flux linkage is decreasing ($e_m < 0$):

(ii) The reluctance torque T_r , although relatively small, is responsible for the torque ripple at low speed. Because of the triangular-shaped variation of the stator winding inductance, the reluctance torque will have a zero average value if the current amplitude is kept constant during one stroke. However, the net reluctance torque will be non-zero if the current is varying;

(iii) The armature reaction field energy W_f, which is to be recovered during current commutation, is very small because of the small value of the stator inductance. Therefore, the energy conversion ratio is very high.

It is clear that at low speed, the DSPM motor is, in principle, similar to the PM brushless DC (PM-BLDC) motor with a 120^0 quasi-square current waveform. The only difference is that the two 120^0 conducting current blocks are drawn together in the case of the DSPM motor. It should be realized that a sufficient interval between the two current blocks must be provided in the design of the DSPM motor to ensure current reversal. At high speed, the current cannot be maintained constant due to the excessive PM induced back EMF. In this case the current peaks in the first half stroke where the inductance is increasing and drops rapidly in the second half stroke where the inductance is decreasing. This uneven distribution of the phase current, however, gives rise to a considerable amount of reluctance torque which ultimately contributes to extending the constant power capability of the DSPM motor. This performance advantage clearly distinguishes the DSPM motor from the PM BLDC motor.

It is interesting to compare the torque production of the DSPM motor with that of the conventional VRM. In this case, both machines are assumed to have identical main dimensions and stator windings. To visualize the difference

between the VRM and the DSPM motor, it is helpful to look at the flux vs. current loci for both motors, as shown in Fig. 4. Two cases are shown in the graph, one for slightly saturated machines (small machines) and the other for highly saturated machines (large machines). To generate the same heat in the two motors, the stator current for the DSPM motor is scaled down to $\sqrt{2}/2$ of that for the VRM. The torque produced in one stroke is represented by the area W for the VRM and W' for the DSPM machine. The area W' is clearly much greater than W due to the fact that: (i) The restored field energy is only a small fraction of the total field energy; (ii) The turn-off angle can be pushed much closer to the aligned position due to the smaller inductance encountered; (iii) Bi-directional operation brings about a handsome gain in torque production. Assuming the same flux swing, it is very clear that the DSPM motor can achieve ideally $\sqrt{2}$ to $2\sqrt{2}$ times the torque density of that of the VRM, depending upon how much the SRM suffers from the excitation penalty.

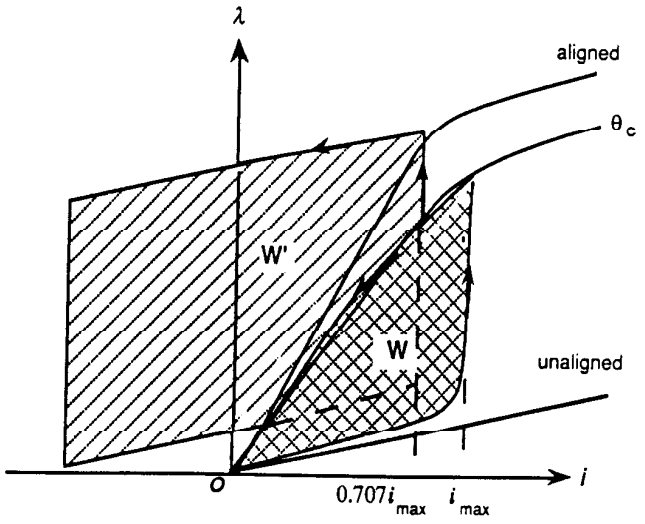

(a) With slight saturation

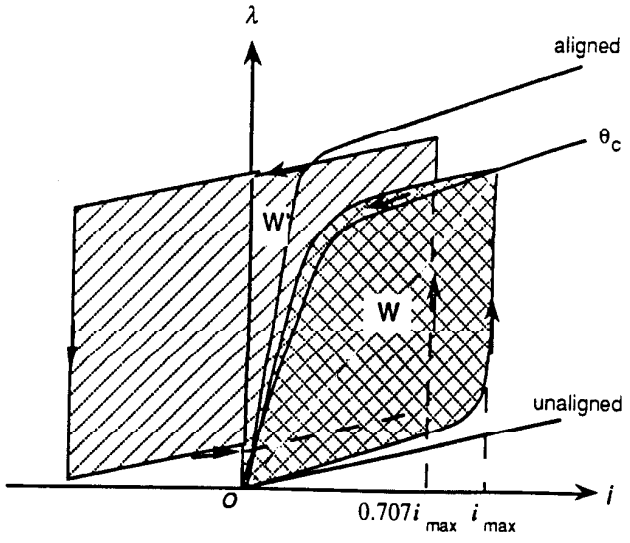

(b) With deep saturation

Fig. 4 Comparison of Torque Production between the VRM and the DSPM Motor

2.3 *Control of the DSPM Motor Drive*

The DSPM motor is flexible with regard to converter selection and can be powered either by one of the unipolar converters as typically used for VRMs [6], or by a bipolar converter as used for PM-BLDC motors [14]. Figure 5 shows a preferred bipolar converter topology with a neutral line to accommodate the additional current which must flow during the commutation period. The DSPM motor drive, as shown schematically in Fig. 5, also features a shaft angle transducer to provide rotor position information for control of the stator currents in the normal manner.

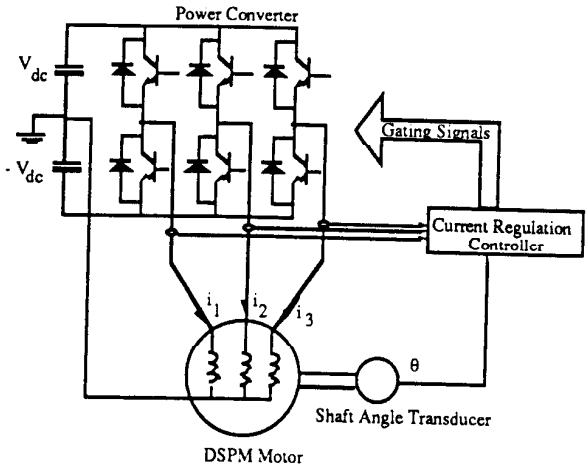

Fig. 5 Schematic Diagram of the DSPM Motor Drive

Control of the DSPM motor is similar to that of the PM-BLDC motor. Four quadrant operation is readily achieved by changing the sequence of conduction and the polarity of the stator currents. Below the base speed, current regulation is preferred to achieve smooth torque production. Above the base speed, the motor becomes voltage fed. Angle control is then utilized in order to realize a constant power range, much the same as that of the VRM.

III. NONLINEAR ANALYSIS OF THE DSPM MOTOR

3.1 *Nonlinear Magnetic Analysis*

Finite Element Analysis (FEA) is an important tool for accurate steady state modeling and performance analysis of the DSPM machines, accounting for magnetic saturation, fringing and demagnetization. In [15], the finite element method was applied to the computation of the two dimensional magnetic field distribution in the cross section of a DSPM machine. The field solution data was then processed to be used for prediction of dynamic and steady state characteristics of the motor. Experience has shown, however, that the gains by using FEA in the DSPM machine, which has relatively simple geometry, are usually small as compared to the more conventional nonlinear magnetic circuit approach (MCA), particularly for small machine where magnetic saturation is not very severe [16]. It has also been shown that for small frame-size machines, the cross-coupling between the PM flux and the armature reaction flux is quite weak, so that the variations of the PM flux linkage and the armature reaction flux linkage can be assumed to be spatially dependent only [16].

Nonlinear magnetic circuit analysis is applied alternatively for this machine topology to calculate the PM flux linkage and phase inductance variations for purposes of design and dynamic analysis. The no-load PM nonlinear magnetic circuit calculation is quite simple [14]. Calculation of the stator winding inductances is based on the computation of the airgap permeance for given rotor position, which is well-established [16]. The effect of local saturation, when desired, can also be introduced in the calculation of the phase inductance with slight modification, especially for the calculation of the maximum inductance with which the armature reaction is greatest.

As a further simplification, curve-fitting techniques can be used to construct the variations of the PM flux linkage and the armature reaction flux linkage from the calculated values at typical rotor positions, following a similar approach as proposed by Miller for the VRM [17]. Positions of interest include the unaligned, aligned, maximum and minimum inductance positions, etc. As shown in Fig. 6, the variation of a typical phase inductance can be approximated by a piece-wise smooth function:

$$f_1(\theta_r) = L_o + \frac{a(\theta_r - \overline{\theta})}{b - (\theta_r - \overline{\theta})}; \qquad 0 \le \theta_r \le \overline{\theta}$$

(Fröhlich-like)

$$f_2(\theta_r) = L_{max} - c(\theta_r - 2\overline{\theta})^2; \qquad \overline{\theta} \le \theta_r \le 2\overline{\theta}$$

(Parabolic)

$$f_3(\theta_r) = \frac{L_{max} - L_{com}}{2} \cos\left(\frac{\pi}{\overline{\theta}}(\theta_r - 2\overline{\theta})\right) + \frac{L_{max} + L_{com}}{2}; \qquad 2\overline{\theta} \le \theta_r \le 3\overline{\theta}$$

$$f_4(\theta_r) = L_{com}. \qquad 3\overline{\theta} \le \theta_r \le 3\overline{\theta} + \delta$$

where a, b, c can be found from continuity constraints.

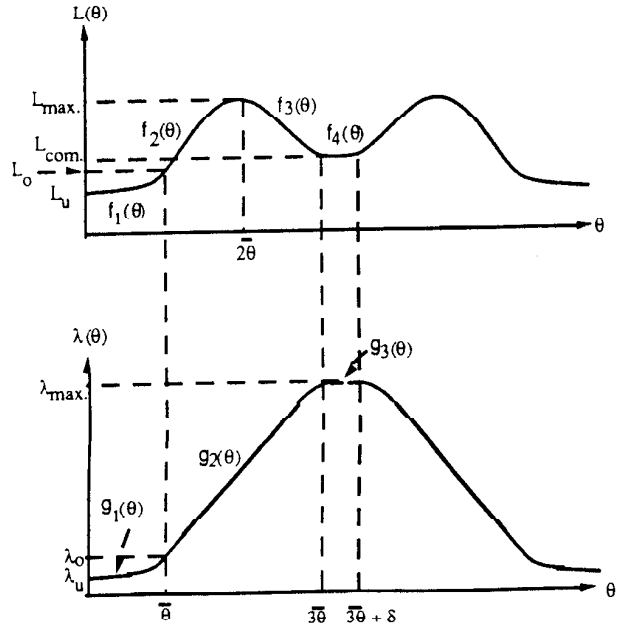

Fig. 6 Variation of (a) the PM Induced Flux Linkage and (b) the Winding Inductance of the DSPM Motor

The PM induced flux linkage variation can then be approximated by a parabolic and straight lines:

$$g_1(\theta_r) = \lambda_o + \frac{a(\theta_r - \overline{\theta})}{b - (\theta_r - \overline{\theta})}; \qquad 0 \le \theta_r \le \overline{\theta}$$

(Fröhlich-like)

$$g_2(\theta_r) = \lambda_{max} - c(\theta_r - 3\overline{\theta}); \qquad \overline{\theta} \le \theta_r \le 3\overline{\theta}$$

$$g_3(\theta_r) = \lambda_{max} \qquad \overline{\theta} \le \theta_r \le 3\overline{\theta} + \delta$$

where a, b, c can be found from continuity constraints.

3.2 Dynamic Simulation

The dynamic model of the DSPM motor is derived in the stationary reference frame in phase quantities, with special accounting for the PM induced flux. The voltage and flux equations describing the motor are, in matrix form, as follows,

$$\underline{V} = \underline{R}\,\underline{I} + \frac{d\underline{\Lambda}}{dt} = \underline{R}\,\underline{L} + \underline{E} \qquad (8.a)$$

where

$$\underline{V} = \begin{pmatrix} v_1 \\ v_2 \\ v_3 \end{pmatrix}, \quad \underline{I} = \begin{pmatrix} i_1 \\ i_2 \\ i_3 \end{pmatrix}, \quad \underline{E} = \begin{pmatrix} e_1 \\ e_2 \\ e_3 \end{pmatrix}$$

and

$$\Lambda = \underline{L}\,\underline{I} + \Lambda_m \qquad (8.b)$$

with

$$\underline{L} = \begin{pmatrix} L_{1s} & L_{12} & L_{13} \\ L_{21} & L_{2s} & L_{23} \\ L_{31} & L_{32} & L_{3s} \end{pmatrix}, \quad \underline{R} = \begin{pmatrix} \mathcal{R}_1 & 0 & 0 \\ 0 & \mathcal{R}_2 & 0 \\ 0 & 0 & \mathcal{R}_3 \end{pmatrix}, \quad \Lambda_m = \begin{pmatrix} \lambda_{m1} \\ \lambda_{m2} \\ \lambda_{m3} \end{pmatrix}$$

$\underline{L}$ and Λ_m are assumed to be spatially dependent only, invariant of the stator currents. Note that in contrast to the variable reluctance machine mutual inductances appear on the off diagonal of $\underline{L}$.

From the co-energy method, the equation for the electromagnetic torque can be written as:

$$T_e = \frac{\partial w'}{\partial \theta_r} = \frac{\partial}{\partial \theta_r}\left[\frac{1}{2}\underline{I}^T \underline{L}\,\underline{I} + \Lambda_m^T \underline{I}\right]$$

$$= \frac{1}{2}\underline{I}^T\left(\frac{\partial}{\partial \theta_r}\underline{L}\right)\underline{I} + \left(\frac{\partial}{\partial \theta_r}\Lambda_m\right)^T \underline{I} \qquad (9)$$

The first term in (9) represents the reluctance torque due to variation of the inductances, and the second term is the reaction torque due to interaction between the winding current and the PM flux.

Equation (8) can be expressed explicitly in terms of either flux linkages or currents to be solved by numerical integration. Note that the elements in the inductance matrix and PM flux linkage vector are all position-dependent quantities as given in Section 3.1. The evaluation of torque as per (9) also requires the derivatives of the inductance matrix and PM flux linkages which can be obtained easily from the inductance and flux linkage expressions as given in Section 3.1.

The waveforms of applied voltage and current of a stator phase winding (v_a, i_a) of the prototype DSPM motor

and the instantaneous torque produced (T_e) obtained by dynamic simulation for speeds below and above the base speed are shown in Figs. 7-8. The variation of the PM induced flux (Phia) and the winding inductance (Leaka) is also shown in the figures. The phase current is kept constant by chopping at low speed. The reluctance torque, as a result, causes a ripple on the top of the torque profile. The build-up and decay of phase currents, especially during the commutating period, contribute to the spikes in the torque waveform. At high speed, the inverter voltage is constant and the active phase winding is turned on at an advanced angle to bring the current to a permissible peak value before the pole pair begins to overlap. The current then begins to collapse, followed by a successful current reversal at the aligned position. The torque ripple content is obviously substantial, but the motor can clearly produce a substantial amount of average torque.

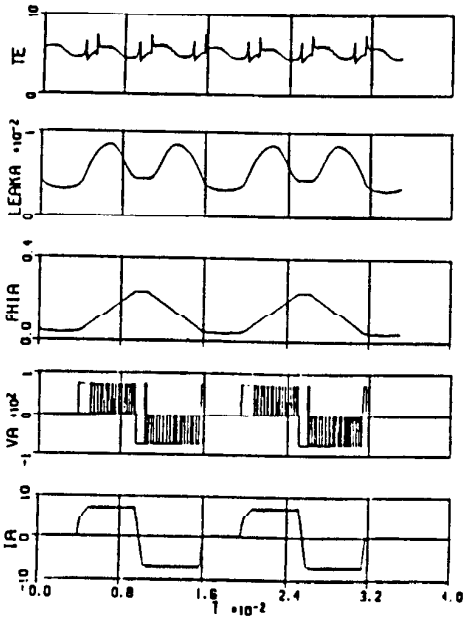

Fig. 7 Simulated Waveforms at Low Speed

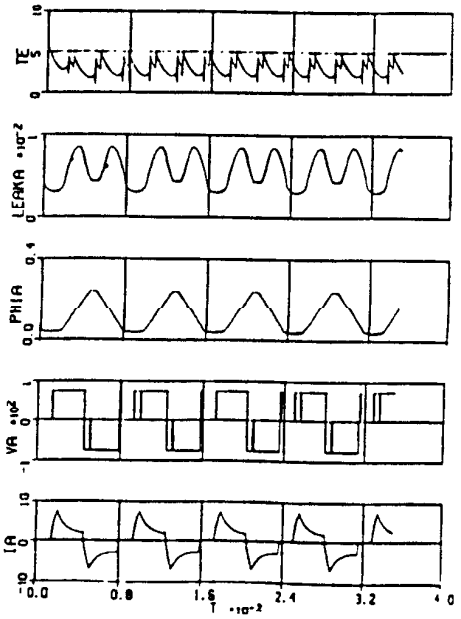

Fig. 8 Simulated Waveforms at High Speed

VI. DESIGN AND PERFORMANCE OF THE PROTOTYPE DSPM MACHINE

A prototype DSPM motor has been designed to support the theory outlined above. Design of the DSPM motor is based on a per phase equivalent circuit similar to Fig. 3, with the inclusion of various practicalities [16]. For a meaningful comparison the prototype machine was designed to have the same outer diameter of stator lamination as that of a 1.0 horsepower induction motor made by Marathon Electric Co. The frames for both machines are NEMA 143 frames. High energy rare earth permanent magnet material Magnequench II is used. The laminated steel used is 24 Gauge, M19 AISI grade.

The stack length of the DSPM Motor is different from the induction machine mainly to accommodate the magnet pieces which are of standard length. The airgap is set to be 0.50 mm. The optimal ratio of OD/ID is determined as a result of a design optimization using a nonlinear programming algorithm termed Sequential Quadratic Nonlinear Programming, with the objective function set to be the torque density and the per unit area copper loss the constraint [16]. The per unit area stator copper losses in both motors are kept almost the same to place both motors under the same cooling conditions. Construction of the prototype DSPM motor and the testing of the whole drive is underway. However, only design and simulation results can be reported here for performance comparison.

Table I summarizes the major performance indices of the prototype motor as against the 1 hp Marathon induction motor. It can be seen that with only 3/5 the stack length of the induction machine, the present motor exceeds the induction machine in torque production, with the efficiency greatly improved. The torque-to-inertia ratio of the DSPM motor is also very impressive as can be noted from Table I.

To fully appreciate the potential of the DSPM motor, two other projected designs are also included in the Table. Design I (DSPM-I), having the same stack length as that of the induction machine, is shown to be able to produce twice the torque as produced by the induction machine, accompanied by an further increased efficiency. Design II (DSPM-II) is set to have the same overall length as that of the induction machine, with the stack length exceeding that of the induction machine. The DSPM motor can then deliver about 2.5 times the torque and power as that of the induction machine housed in the same frame size.

TABLE I
PERFORMANCE COMPARISON BETWEEN THE INDUCTION MOTOR AND DSPM MOTOR

	DSPM Motor	Induction Motor	DSPM-I (projected)	DSPM-II (projected)
Stator OD (mm)	150.	150.	150.	150.
Stack (mm)	30.	47.7	47.7	64.
Airgap (mm)	0.50	.30	.50	.50
Overall Length (fan & brgs excl.)	48.	82.	66.	82.
$P_{cu\text{-}sta}$(watts)	63.1	114.	90.5	109.
P_{loss} (watts)	101.4	232	146.	175.
Efficiency (%)	90.5	75.0	91.1	91.5
Torque (N-M)	5.05	3.96	7.94	9.84
(%)	**128**	**100**	**200**	**248**
Torque/Current (%)	134	100	134	134
Torque/Inertia (%)	554	100	554	554

The average output torque can be evaluated by dynamic simulation as described above. The capability curve of the prototype DSPM motor is shown in Fig. 9, demonstrating this motor can operate with constant power up to 2 times the base speed. The peak current in each phase was limited to 7.5 Amps during the entire speed range.

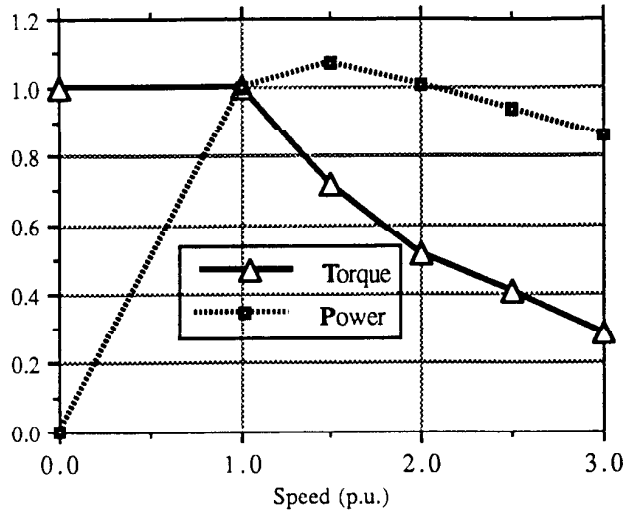

Fig. 9 Torque and Power Capability Curve of the DSPM Motor

V. CONCLUSION

This paper has laid the theoretical foundation for a new type of doubly salient PM machine with stationary permanent magnets. The design and control of these DSPM machines have also been explored but much research work remains ahead to fully assess the potential of such machines. Although the paper treats cylindrical, rotating-field machines, it is evident that the basic principles of the DSPM machine can be employed with advantage to other type of electromechanical devices such as linear machines, etc.

The major advantages of the DSPM motor are summarized as follows:

- High torque density and high efficiency;
- Simple, rugged structure and high speed capability;
- Small VA rating of the power converter as well as the motor;
- Low inertia and fast response;
- Low torque ripple and low noise.

The DSPM motor is, however, a pulsed-torque motor by nature, just like the VRM. This feature may prevent the motor from being used for applications where torque quality is critical. Also, special consideration should be given to reduce the demagnetization effect of the armature reaction in large machines.

In general, with its superior performance in torque production and with structural simplicity, the DSPM motor drive could serve as a potential alternative to existing servo and industrial AC motor topologies, especially in small frame sizes, for variable speed drives. It is especially suitable for applications where size and weight are critical.

ACKNOWLEDGMENT

The Electrical Power Research Institute (EPRI) is acknowledged for funding of this project. Thanks are also due to Mr. Y. Zhao of UW-Madison for help during construction and testing of the power converter and drive; to Mr. William Dittman of Marathon Electric Co. for providing the details of the induction motor and assisting in building the prototype DSPM machine; to Dr. Nady Boules of GM-Research Lab for kindly providing the permanent magnet material Magnequench II.

REFERENCES

[1] Lawrenson, P.J., Stephenson, J.M., Blenkinsop, P.T., Corda J. and Fulton, N.N., "Variable Speed Switched Reluctance Motors", *Proc. IEE*, pt. B, vol. 127, July 1980, pp. 253-65.

[2] Ray, W.F., Lawrenson, P.J., Davis, R.M., Stephenson, J.M. Fulton, N.N. and Blake, R.J., "High Performance Switched Reluctance Brushless Drives", *IEEE Trans. on Industry Applications*, vol. IA-22, no. 4,pp. 722-30.

[3] Stephenson, J. M., and Blake, R. J., "The Design and Performance of a Range of General - Purpose Industrial SR Drives for 1KW to 110KW", *IEEE IAS Annual Meeting*, 1989, pp. 99-107.

[4] McMinn, S.R., "Control of the Switched Reluctance Machine", in *Switched Reluctance Drives*, IEEE IAS Tutorial, 1990.

[5] Richter, E., "Switched Reluctance Machines for High Performance Operation in a Harsh Environment -- a Review Paper", *International Conference on Electrical Machines*, Cambridge, Massachusetts, August 12-15, 1990.

[6] Hava, A., Blasko, V. and Lipo, T.A.," A Modified C-Dump Circuit for Variable Reluctance Machines", *IEEE IAS Annual Meeting*, 1991, pp. 886-91.

[7] Philips, D.A., "Switched Reluctance Drives: New Aspects", *IEEE Power Electronics Specialist Conference (PESC)*, 1989, pp. 579-584

[8] Philips, D.A., "A Novel High Performance-Low Noise Switched Reluctance Motor." *International Conference on Electrical Machines*, Cambridge, Massachusetts, August 12-15, 1990.

[9] Liang, F., Liao, Y. and Lipo, T.A., "Variable Reluctance Motor with Auxiliary Commutating Winding", Submitted for publication at IAS Annual Meeting, Houston Texas, Oct. 1992.

[10] Torok, V. "Electrical Reluctance Machine", U.S. Patent, 4,349,605, 1982.

[11] Walker, J.H., "The Theory of the Inductor Alternator", *Journal of IEE*, vol. 89, Pt. II, 1942, pp. 227-241.

[12] Lipo, T.A., Liao, Y., "Variable Reluctance Motors with Permanent Magnet Excitation", U.S. Patent , pending.

[13] Lipo, T.A., Liao, Y. and Liang F., "A New Doubly Salient Permanent Magnet Motor with Stationary Magnet", U.S. Patent , pending.

[14] T.J.E. Miller: "*Brushless PM and SR Drives*" , Clarenden Press. 1989.

[15] Liao, Y. and Lipo, T.A., "A New Doubly Salient Permanent Magnet Motor for Adjustable Speed Drives", SPEEDAM, Italy, May, 1992.

[16] Liao, Y., "Design *and Performance Evaluation of a New Class of Permanent Magnet Machines with Doubly Salient Structure*", Preliminary Ph.D. Thesis, UW-Madison, Jan. 1992.

[17] Miller, T.J.E. and McGilp, M., "Nonlinear Theory of the Switched Reluctance Motor for Rapid Computer-Aided Design", *Proc. IEE*, pt. B, vol.137, Nov. 1990, p. 337-45.